HHS Public Access

Author manuscript

Mol Psychiatry. Author manuscript; available in PMC 2017 October 26.

Published in final edited form as:

Mol Psychiatry. 2017 November ; 22(11): 1585–1593. doi:10.1038/mp.2017.3.

Neural mechanisms of mismatch negativity (MMN) dysfunction in schizophrenia

Migyung Lee, M.D., Ph.D.[1,2], **Pejman Sehatpour, M.D., Ph.D.**[1,2], **Matthew J. Hoptman, Ph.D.**[2], **Peter Lakatos, M.D. Ph.D.**[2], **Elisa C. Dias, Ph.D.**[1,2], **Joshua T. Kantrowitz, M.D.**[1,2], **Antigona M. Martinez, Ph.D.**[1,2], and **Daniel C. Javitt, M.D., Ph.D.**[1,2]

[1]Division of Experimental Therapeutics, Department of Psychiatry, Columbia University, New York, NY 10032

[2]Schizophrenia Research Division, Nathan Kline Institute for Psychiatric Research, Orangeburg, NY 10962

Abstract

Schizophrenia is associated with cognitive deficits that reflect impaired cortical information processing. Mismatch negativity (MMN) indexes pre-attentive information processing dysfunction at the level of primary auditory cortex. This study investigates mechanisms underlying MMN impairments in schizophrenia using event-related potential (ERP), event-related spectral decomposition (ERSP) and resting state functional connectivity (rsfcMRI) approaches. For this study, MMN data to frequency, intensity and duration deviants were analyzed from 69 schizophrenia patients and 38 healthy controls. rsfcMRI was obtained from a subsample of 38 patients and 23 controls. As expected, schizophrenia patients showed highly significant, large effect-size ($p=.0004$, $d=1.0$) deficits in MMN generation across deviant types. In ERSP analyses, responses to deviants occurred primarily the theta (4–7 Hz) frequency range consistent with distributed corticocortical processing, while responses to standards occurred primarily in alpha (8–12 Hz) range consistent with known frequencies of thalamocortical activation. Independent deficits in schizophrenia were observed in both the theta response to deviants ($p=.021$) and the alpha-response to standards ($p=.003$). At the single trial level, differential patterns of response were observed for frequency vs. duration/intensity deviants, along with At the network level, MMN deficits engaged canonical somatomotor, ventral attention and default networks, with a differential pattern of engagement across deviant types ($p<.0001$). Findings indicate that deficits in thalamocortical, as well as cortico-cortical, connectivity contribute to auditory dysfunction in schizophrenia. In addition, differences in ERSP and rsfcMRI profiles across deviant types suggest potential differential engagement of underlying generator mechanisms.

Correspondence: Daniel C. Javitt, M.D., Ph.D., Director, Division of Experimental Therapeutics, Professor of Psychiatry and Neuroscience, Columbia University College of Physicians and Surgeons, 1051 Riverside Dr., Unit 21, New York, NY 10032, dcj2113@columbia.edu / javitt@nki.rfmh.org.

Conflict of interest:

The authors describe no conflicts of interest in relation to the work described.

Introduction

Schizophrenia is a severe mental disorder associated with generalized impairments in cognitive function. Deficits involve impairments not only in complex functions such as executive function and working memory but also basic sensory function such as auditory or visual processing (rev. in[1, 2]). Auditory mismatch negativity (MMN) is a neurophysiological biomarker that indexes neural mechanisms underlying cognitive dysfunction in schizophrenia (rev. in[3–7]). Moreover, MMN deficits correlate highly with level of function in established[5, 8], first-episode[9] and prodromal[10, 11] schizophrenia, suggesting that it indexes core pathophysiological mechanisms.

At the neurochemical and anatomical levels MMN has been shown to reflect impaired N-methyl-D-aspartate receptor (NMDAR) function[12–15] at the level of supratemporal auditory cortex in schizophrenia[2, 15–18]. By contrast, ensemble-level processes contributing to MMN impairments have been studied to a lesser degree. The present study uses event-related spectral decomposition (ERSP) analysis of MMN data, combined with resting-state functional-connectivity (rsfcMRI) to investigate processes underlying MMN dysfunction in schizophrenia at both the local and distributed circuit levels.

MMN is generated most frequently by deviant stimuli within an auditory oddball paradigm[3, 19]. In such studies, MMN has traditionally been studied using time-domain event-related potential (ERP) techniques[20–22]. In this approach, MMN is manifest as a negative response over frontocentral scalp that inverts at electrodes below the line of the superior temporal plane, consistent with primary generators within supratemporal auditory cortex (rev. in[23]). A right inferior frontal gyrus (IFG) generator has also been observed to some but not all deviants[23], along with more variably reported generators in parietal and midline frontal regions[24, 25]. In schizophrenia, deficits are observed across deviant types, with deficits in duration and intensity deviants predominating at early stages of the illness and deficits in frequency MMN predominating thereafter[8, 26].

In ERSP analysis, electrophysiological activity is divided conventionally into discrete delta (.5–4 Hz), theta (4–7 Hz), alpha (7–12 Hz), beta (12–24 Hz) and gamma (>24 Hz) bands, which reflect differential underlying local-circuit processes[20, 27–29]. Within these bands, stimulus-related activity is further differentiated into those that reflect alterations in phase reset mechanisms as reflected in intertrial coherence (ITC) vs. those that reflect alterations in single-trial power (e.g.[28, 30]).

In the auditory system, thalamocortical activity maps primarily within the alpha frequency range[31, 32], whereas corticocortical connectivity among neurons with similar stimulus sensitivity is reflected in theta frequency interactions[33]. We[34] and others[35, 36] have previously linked MMN dysfunction in schizophrenia primarily to impaired theta frequency response. In the present study we investigate alpha-frequency activation to standard stimuli as well.

Finally, we utilized rsfcMRI[37] to analyze distributed networks involved in stimulus processing. In schizophrenia, deficits in both thalamocortical[38] and corticocortical[39–41] connectivity have increasingly been tied to cognitive dysfunction[38]. We have also recently

observed that deficits in MMN to emotion-relevant frequency modulated (FM) tones correlates with connectivity impairments between auditory and limbic structures[42]. Here, we perform a similar, distributed network analysis for more traditional MMN measures.

In recent rsfcMRI network analyses, auditory cortex has been found to segregate into a combined auditory/somatomotor network, reflecting the close relationship between auditory and rhythmic processing[43]. In our ERSP analyses, we hypothesized that patients would show deficits in response to standards and deviants in the alpha and in theta frequency ranges, respectively, reflecting combined thalamocortical and corticocortical neurotransmission. In rsfcMRI, we hypothesized that network level impairments to simple deviants (frequency, duration, intensity) would involve primarily somatomotor networks, but potential contributions of remaining networks were investigated as well.

Methods

Participants

Written informed consent was obtained from 69 patients diagnosed with schizophrenia/schizoaffective disorder from inpatient and chronic residential care settings associated with Nathan Kline Institute (Orangeburg, NY) and 38 healthy controls (Table 1). Individuals with organic brain disorders, mental retardation, past drug or alcohol dependence, current drug or alcohol abuse, or hearing/vision impairments were excluded. All procedures were approved by the NKI IRB.

Procedure

Auditory stimuli consisted of a sequence of tones presented in random order with a stimulus onset asynchrony of 500–505 ms. Standard stimuli (70% sequential probability) were harmonic tones composed of three superimposed sinusoids (500, 1000, and 1500 Hz) 100-ms in duration, ~85 dB, and with 5-ms rise and fall time. Frequency, duration and intensity deviants (10% probability each) were 10% lower in frequency, 50-ms longer in duration and 10 dB lower in intensity, respectively. At the beginning of each run, the first 15 auditory stimuli were standards. Simultaneous visual stimuli were presented as distractors.

Data Acquisition

Continuous EEG data along with digital timing tags were acquired with either a 72- or 168-channel BioSemi Active II system with standard reference and ground procedures. All data were transformed to an 81 reference free montage using BESA prior to analysis and epoched from −500–1000 ms. Epochs with activity exceeding ±100μV were rejected. For ERP analyses, waveforms were averaged by stimulus type and baseline-corrected relative to pre-stimulus baseline. MMN waveforms were determined by subtraction of standard from deviant responses. Standard and MMN responses were assessed at the frontal midline (Fz) electrode relative to mastoids. ERP from a subsample of this study have been published previously[8].

ERSP

ERSP analyses were constructed using two complementary approaches. For evoked analyses, ERP waves were transformed by multitaper method with Hanning window implemented with Fieldtrip Open Toolbox with 10ms time resolution and 1Hz step of frequency resolution[44].

For single-trial analyses, ITC and baseline-corrected single-trial power were obtained from BESA 5.1 using a complex demodulation procedure[45, 46] with 2 Hz frequency resolution and 25ms time resolution. ITC (also termed intertrial phase locking, ITPL) reflects the consistency of spectral response across repeated trials. Values can range from 0 (no consistency) to 1 (perfect consistency). In general, changes in ITC in the absence of alterations in spectral power are thought to reflect stimulus-induced phase reset of ongoing oscillatory activity. Changes in single-trial power may be either tightly ("evoked") or loosely ("induced")[20] locked to the phase of the eliciting stimulus. Induced activity is thus observed in power plots in the absence of corresponding alterations in ITC.

rsfcMRI acquisition—Scanning took place on the Siemens (Erlangen, Germany) 3T TiM Trio or 1.5T Vision Scanner. For 3T, participants (n=37 patients/14 controls) received an MPRAGE (TR = 2500 ms, TE = 3.5 ms, TI = 1200 ms, matrix=256×256, FOV=256, slice thickness=1mm, 192 slices, no gap, 1 acquisition), and a 5 to 6 minute rsfcMRI scan (TR=2000 ms, TE=30ms, matrix=96×96, FOV=240 mm,2.8 mm slice thickness, 34–36 slices, 0.7 mm gap, 180 acquisitions, IPAT=2) using either a 12- or 32-channel head coil. For 1.5T, participants (3 patients/3 controls) received an MPRAGE T1-weighted scan (TR=11.6 ms, TE=4.9ms, TI=1122ms, matrix=256×256, FOV=256 mm, slice thickness=1 mm, 190 slices, no gap, 1 acquisition), and a five or six minute rsfcMRI scan (TR=2000 ms, TE=50 ms, matrix=64×64, FOV=224 mm, 5 mm slice thickness, 22 slices, no gap, 180 acquisitions). For rsfcMRI, participants were instructed to close their eyes and remain awake. Research study staff confirmed that subjects remained awake after each scan.

Assessment of functional connectivity at resting state in fMRI—rsfcMRI data were preprocessed using DPARS/DPABI, version 1.3 as described elsewhere in detail[47]. Briefly, the first 5 volumes were discarded to eliminate T1 relaxation effects and time series were truncated to a maximum length of 145 scans. Motion correction was then performed. Functional images were then registered to a standard space echo planar template that comes with SPM distribution, and tissue-type segmentations were derived from anatomical "prior" images in standard space. Nuisance regressors were then removed[48], including motion parameters and their derivatives, global, white matter, CSF time series, and linear and quadratic trends. Data were smoothed with a 6 mm Gaussian kernel and filtered (0.1–0.01Hz). Because small volume-to-volume movements can influence rsfcMRI results[49], we computed framewise displacement (FD)[50]. Two patients whose FD values were more than 2 sd above the overall mean was dropped from analyses[48]. The final sample (38 patients/23 controls) did not differ in FD (t_{59}=0.30, p =.76).

Regions of interest (ROIs) were placed in bilateral Heschl's gyrus (HG) and planum temporale (PT) as described elsewhere in detail[47]. We conducted voxelwise general linear

model (GLM) analyses for the auditory cortex ROIs, controlling for magnet (1.5/3T) and FD incorporating group difference contrasts. Additional models were created using MMN variables as covariates of interest to examine relationships between HG/PT connectivity and MMN amplitudes. The GLM analyses produced thresholded z-statistic maps of clusters defined at a z-threshold of 2.3 and a corrected cluster threshold of p=0.05 using Gaussian Random Field theory.

Clinical Measures—Positive and Negative Syndrome Scale (PANSS)[51] scores were obtained from a subset of patients.

Statistical Analysis—The sample size was selected to permit detection of moderate (d=.5) effect size between-group differences, as well as moderate (r=.3) effect-size correlations between variables in the schizophrenia group. Primary between-group comparisons were analyzed using repeated measures multivariate analysis of variance (rmMANOVA) with within-subject factor of deviant type (frequency, intensity, duration) and between-subject factor of diagnostic group. Relationship of MMN amplitude to specific predictor variables was assessed using multiple regression analyses with group included as a factor.

All statistics were two-tailed with preset alpha level for significance of $p<.05$. ERP amplitude values were arc-tangent transformed to increase distributional normality. Between-group homogeneity of variance was assessed using Levene's test, and non-parametric tests were used if required to confirm statistical effects. Values in text are mean ± sem unless otherwise indicated.

Results

ERP/ERSP data analyses were obtained from the full sample of subjects (Table 1). rsfcMRI were additionally obtained from a subset of subjects and correlated with MMN results.

Response to deviants

ERP—As expected, patients showed significant deficits in MMN generation across deviant types ($F_{1,105}=15.5$, p=.0001, d=.82) with no significant group-by-deviant type interaction ($F_{2,104}=.64$, p=.53). Between-group differences were independently significant for each MMN type (Fig 1A). MMN latencies were also shorter for patients than controls ($F_{1,105}=8.85$, p=.004) with no significant group-by-deviant interaction ($F_{2,104}=1.18$, p=.3) (Supplementary Table 1).

ERSP—In evoked power analysis, MMN corresponded to an increase in evoked power centered within the theta frequency band (Fig. 1B). Theta-power deficits in schizophrenia were significant across deviant types ($F_{1,104}=5.59$, p=.02) with no group-by-deviant type ($F_{2,103}=1.17$, p=.32) interaction (Fig. 1C).

In single trial analyses, ERSP were decomposed into separate single-trial power (Fig 1D) and ITC (Fig 1E). Significant reductions were observed in both theta-frequency power ($F_{1,105}=8.41$, p=.005) and ITC ($F_{1,105}=9.12$, p=.003) across deviant types. However, for frequency MMN, between group differences in ITC were no longer significant following co-

variation for changes in power ($F_{1,104}$=2.12, p=.15). By contrast, for intensity ($F_{1,104}$=7.07, p=.009) and duration ($F_{1,104}$=3.83, p=.05) deviants, significant deficits in ITC remained.

Response to standards

ERP—Consistent with prior literature, time domain responses to standard stimuli were characterized by a small P1/N1 response that was not significantly different between groups (t_{102}=.2, p=.8) (Fig. 2A).

ERSP—As predicted, standard stimuli elicited a well circumscribed increase in alpha power that was significantly reduced in patients (t_{105}=3.22, p=.002, d=.63)(Fig. 2B). In single-trial analyses, reductions were observed in both single-trial power (t_{105}=3.22, p=.002, d=.63) (Fig. 2C) and ITC (t_{105}=3.89, p=.0002, d=.76) (Fig. 2D). As opposed to evoked power, ITC responses spread to the theta frequency range, where a reduction in ITC was also observed (t_{105}=3.17, p=.002) (Fig. 2D).

As opposed to the increase in theta ITC, both groups showed a stimulus-induced reduction in theta power to standard stimuli that was significantly diminished in patients relative to controls (t_{105}=−3.13, p=.002) (Fig. 2C). When responses to standards were entered into the discriminant stimulus function along with responses to deviants, both alpha ITC ($F_{1,105}$=15.2, p<.0001) and single-trial theta power suppression ($F_{5,101}$=6.57, p<.001) contributed along with MMN-related theta increases to differentiation between patients and controls.

Network level analysis

rsfcMRI analyses were performed relative to seeds placed in primary (HG) and secondary (PT) auditory regions. As expected, patients showed significantly reduced local connectivity across all 4 seeds ($F_{1,59}$=6.43, p=.014) with significant deficits for both HG ($F_{1,59}$=7.84, p=.014) and. PT ($F_{1,59}$=4.90, p=.031) seeds (Fig. 3A). Reduced connectivity correlated within the auditory regions correlated significantly with theta power increases to frequency-deviants across groups for all seeds (all p<.01) with strongest correlation for right HG (r=.37, p=.003). This correlation remained significant in patients alone (r=.36, p=.027).

When analyses were expanded outside of auditory cortex, additional correlation regions were observed outside of classic auditory regions. In order to determine the functional basis for this distribution, correlation regions were mapped onto rsfcMRI network maps derived from the Human Connectome Project[37] (Fig. 3C,D).

For all deviants, the large majority of correlated voxels fell within the combined auditory/somatomotor (Fig. 3E). Within this network, however, correlated voxels for frequency MMN was confined largely to core auditory regions, especially on the right (Fig. 3D, arrow). By contrast, intensity/duration-deviants engaged somatomotor networks more generally, with extensive correlations within somatomotor regions corresponding to face, hand, and foot regions of the classic homunculus.

In addition, frequency-deviants uniquely engaged “default mode” regions of inferior auditory cortex, whereas for intensity/duration-deviants, additional voxels were observed in ventral attention networks that are thought to contribute to processing of stimulus salience.

The pattern of engagement was highly significant across deviants (χ^2_{12}=2270, p<.0001), suggesting significant differential patterns of network-level cortical engagement. No significant engagement of limbic or frontoparietal networks was observed for any of the deviants used in this study.

Correlations with clinical features, age and premorbid function

Demographic variables—As in earlier studies[8], MMN amplitude correlated significantly with premorbid education (Fig. 4A) even after controlling for group status ($F_{1,84}$=11.8, p=.001), with greatest correlation for intensity MMN (partial r=−.35, p=.001). Amplitudes of intensity (r=.23, p=.016) and duration (r=.22, p=.026). In order to evaluate the degree to which the correlations were the same in patients vs. controls, we performed a follow-up ANOVA in which we explicitly modeled the group × education interaction across the three deviant types. As in the initial analysis, the correlation with education status was significant across groups ($F_{3,81}$=4.40, p=.006). As expected, neither the main effect of group ($F_{3,81}$=.47, p=.7) nor the group × education interaction was significant ($F_{3,81}$=.59, p=.6), demonstrating a similar correlation across groups.

MMN also declined significantly with age, with correlations remaining significant even following control for group status (duration: partial r=.29, p=.048; intensity: partial r=.21, p=.034). By contrast, correlations with frequency MMN vs. age were not statistically significant (partial r=.14, p=.14). In a follow-up analysis assessing similarity in strength of correlation across group, we modeled the group × age interaction. In this analysis, the correlation with age remained significant ($F_{1,102}$=6.28, p=.014), while the group × age interaction was not significant ($F_{1,102}$=1.87, p=.18).

When the correlations were analyzed according to underlying process, a significant overall relationship was observed between ITC measures and age ($F_{1,103}$=2.99, p=.034) and independently for intensity (r=−.20, p=.037) and duration (r=−.28, p=.004) (Fig. 4B) By contrast, no significant relationship was observed between single-trial power and age either across deviants ($F_{1,103}$=.01, p=.9) or for individual deviants. No significant correlations were observed between age and responses to standard stimuli.

Symptoms—No correlations were observed between symptoms and ERP measures to either standards or deviants. By contrast, theta power inhibition to standards correlated significantly with severity of positive symptoms in general (r_{66}=−.34, p=.004)(Fig. 4C) and hallucinations (r_{43}=−.44, p=.003), delusions (r_{43}=−.33, p=.038) and persecution (r_{43}=−.43, p=.005), with more suppression correlating with greater severity. ITC to duration-deviants also correlated strongly with positive symptom severity (r_{66}=−.38, p=.002) (Fig. 4D) but only the correlation with delusions was independently significant (r_{43}=−.33, p=.038).

Medication—No significant correlations were observed to negative or cognitive symptoms, or to medication dosage as reflected in CPZ equivalents.

Discussion

Deficits in MMN generation were first demonstrated over 20 years, and since then have become among the most widely replicated neurophysiological indices of cortical dysfunction in schizophrenia (rev in.[5, 6, 52]). Deficits in MMN generation predict poor functional outcome not only in schizophrenia[8] but even in otherwise healthy adults[53]. Furthermore, deficits are reliably reproduced across deviant types by administration of NMDAR antagonists[18, 54] but not other psychotomimetics[55].

At the process level, MMN depends upon the ability of auditory cortex to create and maintain a short-term auditory memory based upon presentation of repetitive standard stimuli and then to detect deviations in regularity patterns induced by the deviants - a process initially termed “primitive intelligence”[56] but more recently reconceptualized as NMDAR-linked “prediction error” within auditory cortex[57–61]. MMN represents the outcome of this process, and is thus a reliable index of information processing dysfunction at the level of auditory cortex in schizophrenia.

MMN studies in schizophrenia to date, however, have been limited by the inability of traditional time-domain MMN analysis to resolve the responses to the standard stimuli within the MMN sequence, due to the small amplitude of these responses relative to overlapping sources of neural activity. Responses to the standard stimuli are critical to establishing the mnemonic template underlying the intracortical MMN process. In order to isolate these responses, the present study utilizes an ERSP (“time-frequency”) approach to isolate responses to standards in frequency as well as time.

As predicted[62, 63], responses to standard stimuli were dramatically reduced in patients, along with responses to deviants, suggesting impaired input to auditory cortex as well as impaired local processing within auditory cortical networks. In addition, ERSP analyses showed significant differential mechanisms underlying responses to different deviant types. Finally, rsfcMRI demonstrated significant engagement across somatomotor and attentional networks, supporting distributed mechanisms of MMN deficits in schizophrenia.

Theta frequency and ensemble activity within auditory regions

Deficits in auditory gamma-frequency response in schizophrenia have been extensively documented using paradigms such as steady-state response, which are related to impaired function of parvalbumin (PV)-type inhibitory interneurons (e.g.[64]). By contrast, we[34] and others[35, 36,65] have linked MMN deficits to impaired theta-frequency response, and underlying NMDAR dysfunction in rodent[66, 67] and primate[28] models. At the local circuit level, theta rhythms are tied to interactions involving non-PV cells, especially somatostatin-type inhibitory interneurons[6, 29, 68]. The present replication of prior theta-frequency findings thus further supports models of impaired function across interneuron types in schizophrenia[6].

In addition, our present findings provide the first evidence that MMN generation to different deviant types is associated with a differential underlying mechanism both in schizophrenia patients and healthy controls. Thus, whereas frequency MMN deficits were associated

primarily with reductions single-trial power (as also reported previously[65]), intensity MMN deficits were associated exclusively with reductions in ITC, while duration MMN showed mixed contributions (Fig. 1D,E).

At present the basis for these differences is unknown, However, it is noteworthy that these observations converge with differentiation of the auditory thalamus (medial geniculate nucleus, MGB) into histologically distinct core and matrix subdivisions (lemniscal/non-lemniscal), as first described by Jones (e.g.[69–71]). In this schema, core neurons are tonotopically organized, project narrowly to primary and secondary auditory cortical regions, and provide “driving” inputs that induce net current flow (single-trial power) along with phase reset of auditory cortical neurons[72].

By contrast, matrix neurons show poor frequency sensitivity, but strong sensitivity to variations in the intensity and pattern of auditory inputs[73], and act primarily as modulators, rather than drivers, of cortical[72]. As such, these projections induce alterations primarily in ITC as observed for intensity/duration MMN.

In this study, as well as prior research[8, 26, 52], the age trajectory differed significantly between frequency and intensity/duration MMN. Follow up analysis, however, demonstrated that the difference was due specifically to the significant age-dependence of theta ITC across deviant types vs. lack of age effect on power, suggesting that differential aging effects on thalamic subsystems may contribute to the differential age relationships for MMN deficits in schizophrenia.

Recent fMRI studies also suggest significant deviance-related activity within both MGB and inferior colliculus[74] in healthy subjects, consistent with present results. Future studies utilizing high-field (7T) fMRI may have resolution sufficient to evaluate differential involvement of MGB nuclei in different MMN types[75] as well as neural mechanisms underlying impairments in schizophrenia.

Response to standards

In contrast to the theta-frequency MMN response, responses to the standard stimuli occurred primarily within the alpha frequency band, and were associated with active inhibition of theta activity. Deficits in response to standards were not detected in traditional ERP assessment (Fig. 2A). By contrast, in ERSP analyses robust deficits were observed (Fig. 2B) that were manifest at the level of both single-trial power and ITC (Fig. 2C,D).

Our finding of isolated alpha-band response to standards is consistent with recent human[31, 33] and primate[32] intracranial recording studies of thalamocortical activity. To our knowledge, however, this is the first study to isolate the alpha response to standards during the MMN paradigm, and thus the first to provide clear evidence of impaired thalamocortical input to cortex in schizophrenia. Of note, the alpha response to standards distinguishes schizophrenia and control subjects over and above impaired MMN generation, suggesting that impairments in establishing the mnemonic template to standards may contribute along with deviance detection to MMN deficits in schizophrenia.

Simultaneous with the increases in alpha power to standards, active suppression was observed in ongoing theta activity and was reduced in schizophrenia (Fig. 2D). Moreover, the degree of dysfunction correlated highly with severity of positive symptoms, including hallucinations, suggesting that theta modulation to standards may represent an additional biomarker for auditory dysfunction related to hallucinatory activity in schizophrenia.

Neural networks

As a complement to ERSP, we used rsfcMRI data to analyze distributed neural circuits underlying impaired MMN generation. In patients, reduced functional connectivity was observed in a network involving primary (HG) and secondary (PT) auditory cortex for all 3 deviant types. However, additional differential correlation regions were also observed. Most notably, significant correlations were observed across the entire somatomotor network, which plays a critical role in processing of rhythmicity.

These correlations extended even over the convexity and may contribute to recently reported MMN deficits within dorsal and parietal regions in schizophrenia[25]. In addition, the networks extended into ventral attention “salience” regions, such as IFG. Neurons within these regions, such as those located in Broca’s language area and Broca’s right homologue, have well-described theta frequency synchronization with auditory cortex[33, 76] that may reflect shared representation of frequency information.

Finally, for MMN to frequency-deviants, we observed extensive correlations with regions in the default mode network, consistent with prior findings elsewhere[39]. As opposed to our recent observations with FM-tone MMN[42], little engagement of limbic regions was observed to deviations in simple tonal features that (unlike FM tones) do not induce an emotional percept.

Limitations

All patients in this study were receiving antipsychotic medication. In general, dopaminergic agents have been found neither to potentiate nor inhibit MMN generation, Moreover, in the present study no correlations was observed with medication dose. Nevertheless, replication in medication free or prodromal groups may be critical. In addition, fMRI and symptom ratings were only obtained in a subset of subjects potentially limiting power to detect relationships.

In addition, hearing thresholds were not obtained in either patients or controls, so potential effects of age-related hearing loss on MMN amplitude across groups could not be determined. Nevertheless, pure tone thresholds are typically intact in schizophrenia[6]. Moreover, although severe hearing loss may affect MMN generation, MMN latencies are typically affected to a greater extent than amplitude[77, 78]. In the present study, all subjects had normal hearing by self-report and reported being able to comfortably hear the presented stimuli. Tones were also lower frequency (<2 kHz) to reduce age-related effects. Most importantly, MMN latencies were similar across groups (Supplemental Table 1) and not correlated with age, suggesting limited contribution of age-related hearing changes to MMN amplitude differences.

Finally, in the present study MMN responses were assessed relative to resting state functional connectivity (rsfcfMRI), rather than connectivity obtained during auditory stimulation. The decision not to use auditory stimulation during functional connectivity scans was made, in part, due to the poor temporal resolution of fMRI relative to ERP, and thus the attendant difficulty in differentiation MMN-related activity from activity related to other auditory potentials that occur prior to and following the MMN peak in the ERP waveform[74, 79]. Moreover, because of the computations involved in determination of functional connectivity, differentiating stimulation-induced changes in connectivity from changes in activation can be challenging, and results must be interpreted with caution[80]. The technique applied in the present study has been advocated across cognitive domains in schizophrenia[41], but has not previously been applied to the study of MMN or other auditory-dependent cognitive impairments. Future studies using task-based fMRI to investigate integrity of cortical/subcortical processing of different deviant types in schizophrenia are therefore required.

Summary

MMN has been extensively studied in schizophrenia using traditional ERP approaches. However, this is the first study of which we are aware to isolate responses to standard-, as well as deviant-, stimuli within the MMN paradigm, and thus to demonstrate reduced thalamocortical activation of cortex to standard stimuli, along with reduced cortico-cortical connectivity to deviants. Differential ERSP and rsfcMRI signatures of frequency vs. intensity/duration MMN and differential age regressions may be related to differential engagement of core vs. matrix subdivisions of auditory thalamus (MGB) by the different deviant types. Future translational imaging studies focused on thalamic mechanisms may provide further insights into neural mechanisms of prediction error deficits in schizophrenia.

Supplementary Material

Refer to Web version on PubMed Central for supplementary material.

Acknowledgments

Supported by USPHS grants MH49334 and MH109289 to DCJ and MH064783 and MH084031 to MJH.

References

1. Javitt DC. When doors of perception close: bottom-up models of disrupted cognition in schizophrenia. Annual review of clinical psychology. 2009; 5:249–275.
2. Javitt DC, Freedman R. Sensory processing dysfunction in the personal experience and neuronal machinery of schizophrenia. Am J Psychiatry. 2015; 172(1):17–31. [PubMed: 25553496]
3. Javitt DC. Intracortical mechanisms of mismatch negativity dysfunction in schizophrenia. Audiol Neurootol. 2000; 5(3–4):207–215. [PubMed: 10859415]
4. Hay RA, Roach BJ, Srihari VH, Woods SW, Ford JM, Mathalon DH. Equivalent mismatch negativity deficits across deviant types in early illness schizophrenia-spectrum patients. Biol Psychol. 2015; 105:130–137. [PubMed: 25603283]
5. Light GA, Naatanen R. Mismatch negativity is a breakthrough biomarker for understanding and treating psychotic disorders. Proc Natl Acad Sci U S A. 2013; 110(38):15175–15176. [PubMed: 23995447]

6. Javitt DC, Sweet RA. Auditory dysfunction in schizophrenia: integrating clinical and basic features. Nat Rev Neurosci. 2015; 16(9):535–550. [PubMed: 26289573]
7. Naatanen R, Sussman ES, Salisbury D, Shafer VL. Mismatch negativity (MMN) as an index of cognitive dysfunction. Brain Topogr. 2014; 27(4):451–466. [PubMed: 24838819]
8. Friedman T, Sehatpour P, Dias E, Perrin M, Javitt DC. Differential relationships of mismatch negativity and visual p1 deficits to premorbid characteristics and functional outcome in schizophrenia. Biol Psychiatry. 2012; 71(6):521–529. [PubMed: 22192361]
9. Salisbury DF, Polizzotto NR, Nestor PG, Haigh SM, Koehler J, McCarley RW. Pitch and Duration Mismatch Negativity and Premorbid Intellect in the First Hospitalized Schizophrenia Spectrum. Schizophr Bull. 2016
10. Carrion RE, Cornblatt BA, McLaughlin D, Chang J, Auther AM, Olsen RH, et al. Contributions of early cortical processing and reading ability to functional status in individuals at clinical high risk for psychosis. Schizophr Res. 2015; 164(1–3):1–7. [PubMed: 25728833]
11. Perez VB, Woods SW, Roach BJ, Ford JM, McGlashan TH, Srihari VH, et al. Automatic auditory processing deficits in schizophrenia and clinical high-risk patients: forecasting psychosis risk with mismatch negativity. Biol Psychiatry. 2014; 75(6):459–469. [PubMed: 24050720]
12. Javitt DC, Zukin SR. Recent advances in the phencyclidine model of schizophrenia. Am J Psychiatry. 1991; 148(10):1301–1308. [PubMed: 1654746]
13. Coyle JT. NMDA receptor and schizophrenia: a brief history. Schizophr Bull. 2012; 38(5):920–926. [PubMed: 22987850]
14. Moghaddam B, Javitt D. From revolution to evolution: the glutamate hypothesis of schizophrenia and its implication for treatment. Neuropsychopharmacology. 2012; 37(1):4–15. [PubMed: 21956446]
15. Gunduz-Bruce H, Reinhart RM, Roach BJ, Gueorguieva R, Oliver S, D'Souza DC, et al. Glutamatergic modulation of auditory information processing in the human brain. Biol Psychiatry. 2012; 71(11):969–977. [PubMed: 22036036]
16. Javitt DC, Steinschneider M, Schroeder CE, Arezzo JC. Role of cortical N-methyl-D-aspartate receptors in auditory sensory memory and mismatch negativity generation: implications for schizophrenia. Proc Natl Acad Sci U S A. 1996; 93(21):11962–11967. [PubMed: 8876245]
17. Gil-da-Costa R, Stoner GR, Fung R, Albright TD. Nonhuman primate model of schizophrenia using a noninvasive EEG method. Proc Natl Acad Sci U S A. 2013; 110(38):15425–15430. [PubMed: 23959894]
18. Rosburg T, Kreitschmann-Andermahr I. The effects of ketamine on the mismatch negativity (MMN) in humans - A meta-analysis. Clin Neurophysiol. 2016; 127(2):1387–1394. [PubMed: 26699665]
19. Mantysalo S, Naatanen R. The duration of a neuronal trace of an auditory stimulus as indicated by event-related potentials. Biol Psychol. 1987; 24(3):183–195. [PubMed: 3663794]
20. Javitt DC, Spencer KM, Thaker GK, Winterer G, Hajos M. Neurophysiological biomarkers for drug development in schizophrenia. Nature reviews. 2008; 7(1):68–83.
21. Luck SJ, Mathalon DH, O'Donnell BF, Hamalainen MS, Spencer KM, Javitt DC, et al. A roadmap for the development and validation of event-related potential biomarkers in schizophrenia research. Biol Psychiatry. 2011; 70(1):28–34. [PubMed: 21111401]
22. Javitt DC. Neurophysiological models for new treatment development in schizophrenia: early sensory approaches. Ann N Y Acad Sci. 2015; 1344:92–104. [PubMed: 25721890]
23. Naatanen R, Kahkonen S. Central auditory dysfunction in schizophrenia as revealed by the mismatch negativity (MMN) and its magnetic equivalent MMNm: a review. Int J Neuropsychopharmacol. 2009; 12(1):125–135. [PubMed: 18771603]
24. Fulham WR, Michie PT, Ward PB, Rasser PE, Todd J, Johnston PJ, et al. Mismatch negativity in recent-onset and chronic schizophrenia: a current source density analysis. PLoS ONE. 2014; 9(6):e100221. [PubMed: 24949859]
25. Rissling AJ, Miyakoshi M, Sugar CA, Braff DL, Makeig S, Light GA. Cortical substrates and functional correlates of auditory deviance processing deficits in schizophrenia. NeuroImage Clinical. 2014; 6:424–437. [PubMed: 25379456]

26. Todd J, Michie PT, Schall U, Karayanidis F, Yabe H, Naatanen R. Deviant matters: duration, frequency, and intensity deviants reveal different patterns of mismatch negativity reduction in early and late schizophrenia. Biol Psychiatry. 2008; 63(1):58–64. [PubMed: 17585889]
27. Makeig S, Debener S, Onton J, Delorme A. Mining event-related brain dynamics. Trends Cogn Sci. 2004; 8(5):204–210. [PubMed: 15120678]
28. Lakatos P, Schroeder CE, Leitman DI, Javitt DC. Predictive suppression of cortical excitability and its deficit in schizophrenia. J Neurosci. 2013; 33(28):11692–11702. [PubMed: 23843536]
29. Womelsdorf T, Valiante TA, Sahin NT, Miller KJ, Tiesinga P. Dynamic circuit motifs underlying rhythmic gain control, gating and integration. Nat Neurosci. 2014; 17(8):1031–1039. [PubMed: 25065440]
30. Lisman JE, Coyle JT, Green RW, Javitt DC, Benes FM, Heckers S, et al. Circuit-based framework for understanding neurotransmitter and risk gene interactions in schizophrenia. Trends Neurosci. 2008; 31(5):234–242. [PubMed: 18395805]
31. Potes C, Brunner P, Gunduz A, Knight RT, Schalk G. Spatial and temporal relationships of electrocorticographic alpha and gamma activity during auditory processing. Neuroimage. 2014; 97:188–195. [PubMed: 24768933]
32. Haegens S, Barczak A, Musacchia G, Lipton ML, Mehta AD, Lakatos P, et al. Laminar Profile and Physiology of the alpha Rhythm in Primary Visual, Auditory, and Somatosensory Regions of Neocortex. J Neurosci. 2015; 35(42):14341–14352. [PubMed: 26490871]
33. Hsiao FJ, Wu ZA, Ho LT, Lin YY. Theta oscillation during auditory change detection: An MEG study. Biol Psychol. 2009; 81(1):58–66. [PubMed: 19428969]
34. Javitt DC, Shelley A, Ritter W. Associated deficits in mismatch negativity generation and tone matching in schizophrenia. Clin Neurophysiol. 2000; 111(10):1733–1737. [PubMed: 11018486]
35. Hong LE, Moran LV, Du X, O'Donnell P, Summerfelt A. Mismatch negativity and low frequency oscillations in schizophrenia families. Clin Neurophysiol. 2012; 123(10):1980–1988. [PubMed: 22541739]
36. Kayser J, Tenke CE, Kroppmann CJ, Alschuler DM, Fekri S, Ben-David S, et al. Auditory event-related potentials and alpha oscillations in the psychosis prodrome: Neuronal generator patterns during a novelty oddball task. Int J Psychophysiol. 2014; 91(2):104–120. [PubMed: 24333745]
37. Yeo BT, Krienen FM, Sepulcre J, Sabuncu MR, Lashkari D, Hollinshead M, et al. The organization of the human cerebral cortex estimated by intrinsic functional connectivity. J Neurophysiol. 2011; 106(3):1125–1165. [PubMed: 21653723]
38. Anticevic A, Gancsos M, Murray JD, Repovs G, Driesen NR, Ennis DJ, et al. NMDA receptor function in large-scale anticorrelated neural systems with implications for cognition and schizophrenia. Proc Natl Acad Sci U S A. 2012; 109(41):16720–16725. [PubMed: 23012427]
39. Whitfield-Gabrieli S, Ford JM. Default Mode Network Activity and Connectivity in Psychopathology. Annual review of clinical psychology. 2011
40. Anticevic A, Cole MW, Murray JD, Corlett PR, Wang XJ, Krystal JH. The role of default network deactivation in cognition and disease. Trends Cogn Sci. 2012; 16(12):584–592. [PubMed: 23142417]
41. Sheffield JM, Barch DM. Cognition and resting-state functional connectivity in schizophrenia. Neuroscience and biobehavioral reviews. 2016; 61:108–120. [PubMed: 26698018]
42. Kantrowitz JT, Hoptman MJ, Leitman DI, Moreno-Ortega M, Lehrfeld JM, Dias E, et al. Neural Substrates of Auditory Emotion Recognition Deficits in Schizophrenia. J Neurosci. 2015; 35(44): 14909–14921. [PubMed: 26538659]
43. Yeo RA, Hodde-Vargas J, Hendren RL, Vargas LA, Brooks WM, Ford CC, et al. Brain abnormalities in schizophrenia-spectrum children: implications for a neurodevelopmental perspective. Psychiatry Res. 1997; 76(1):1–13. [PubMed: 9498305]
44. Oostenveld R, Fries P, Maris E, Schoffelen JM. FieldTrip: Open source software for advanced analysis of MEG, EEG, and invasive electrophysiological data. Computational intelligence and neuroscience. 2011; 2011:156869. [PubMed: 21253357]
45. Papp N, Ktonas P. Critical evaluation of complex demodulation techniques for the quantification of bioelectrical activity. Biomed Sci Instrum. 1977; 13:135–145. [PubMed: 871500]

46. Hoechstetter K, Bornfleth H, Weckesser D, Ille N, Berg P, Scherg M. BESA source coherence: a new method to study cortical oscillatory coupling. Brain Topogr. 2004; 16(4):233–238. [PubMed: 15379219]
47. Hoptman MJ, Antonius D, Mauro CJ, Parker EM, Javitt DC. Cortical thinning, functional connectivity, and mood-related impulsivity in schizophrenia: relationship to aggressive attitudes and behavior. Am J Psychiatry. 2014; 171(9):939–948. [PubMed: 25073506]
48. Yan CG, Cheung B, Kelly C, Colcombe S, Craddock RC, Di Martino A, et al. A comprehensive assessment of regional variation in the impact of head micromovements on functional connectomics. Neuroimage. 2013; 76:183–201. [PubMed: 23499792]
49. Power JD, Barnes KA, Snyder AZ, Schlaggar BL, Petersen SE. Spurious but systematic correlations in functional connectivity MRI networks arise from subject motion. Neuroimage. 2012; 59(3):2142–2154. [PubMed: 22019881]
50. Jenkinson M, Bannister P, Brady M, Smith S. Improved optimization for the robust and accurate linear registration and motion correction of brain images. Neuroimage. 2002; 17(2):825–841. [PubMed: 12377157]
51. Kay SR, Sevy S. Pyramidical model of schizophrenia. Schizophr Bull. 1990; 16:537–545. [PubMed: 2287938]
52. Todd J, Whitson L, Smith E, Michie PT, Schall U, Ward PB. What's intact and what's not within the mismatch negativity system in schizophrenia. Psychophysiology. 2014; 51(4):337–347. [PubMed: 24611871]
53. Light GA, Swerdlow NR, Braff DL. Preattentive sensory processing as indexed by the MMN and P3a brain responses is associated with cognitive and psychosocial functioning in healthy adults. J Cogn Neurosci. 2007; 19(10):1624–1632. [PubMed: 18271737]
54. Umbricht D, Schmid L, Koller R, Vollenweider FX, Hell D, Javitt DC. Ketamine-induced deficits in auditory and visual context-dependent processing in healthy volunteers: implications for models of cognitive deficits in schizophrenia. Arch Gen Psychiatry. 2000; 57(12):1139–1147. [PubMed: 11115327]
55. Umbricht D, Vollenweider FX, Schmid L, Grubel C, Skrabo A, Huber T, et al. Effects of the 5-HT2A agonist psilocybin on mismatch negativity generation and AX-continuous performance task: implications for the neuropharmacology of cognitive deficits in schizophrenia. Neuropsychopharmacology. 2003; 28(1):170–181. [PubMed: 12496954]
56. Naatanen R, Tervaniemi M, Sussman E, Paavilainen P, Winkler I. "Primitive intelligence" in the auditory cortex. Trends Neurosci. 2001; 24(5):283–288. [PubMed: 11311381]
57. Friston K. A theory of cortical responses. Philos Trans R Soc Lond B Biol Sci. 2005; 360(1456): 815–836. [PubMed: 15937014]
58. Garrido MI, Kilner JM, Stephan KE, Friston KJ. The mismatch negativity: a review of underlying mechanisms. Clin Neurophysiol. 2009; 120(3):453–463. [PubMed: 19181570]
59. Todd J, Michie PT, Schall U, Ward PB, Catts SV. Mismatch negativity (MMN) reduction in schizophrenia-impaired prediction–error generation, estimation or salience? Int J Psychophysiol. 2012; 83(2):222–231. [PubMed: 22020271]
60. Wacongne C, Changeux JP, Dehaene S. A neuronal model of predictive coding accounting for the mismatch negativity. J Neurosci. 2012; 32(11):3665–3678. [PubMed: 22423089]
61. Wacongne C. A predictive coding account of MMN reduction in schizophrenia. Biol Psychol. 2016; 116:68–74. [PubMed: 26582536]
62. Butler PD, Martinez A, Foxe JJ, Kim D, Zemon V, Silipo G, et al. Subcortical visual dysfunction in schizophrenia drives secondary cortical impairments. Brain. 2007; 130(Pt 2):417–430. [PubMed: 16984902]
63. Martinez A, Hillyard SA, Dias EC, Hagler DJ Jr, Butler PD, Guilfoyle DN, et al. Magnocellular pathway impairment in schizophrenia: evidence from functional magnetic resonance imaging. J Neurosci. 2008; 28(30):7492–7500. [PubMed: 18650327]
64. Gonzalez-Burgos G, Fish KN, Lewis DA. GABA neuron alterations, cortical circuit dysfunction and cognitive deficits in schizophrenia. Neural Plast. 2011; 2011:723184. [PubMed: 21904685]

65. Kaser M, Soltesz F, Lawrence P, Miller S, Dodds C, Croft R, et al. Oscillatory underpinnings of mismatch negativity and their relationship with cognitive function in patients with schizophrenia. PLoS ONE. 2013; 8(12):e83255. [PubMed: 24358266]

66. Lazarewicz MT, Ehrlichman RS, Maxwell CR, Gandal MJ, Finkel LH, Siegel SJ. Ketamine modulates theta and gamma oscillations. J Cogn Neurosci. 2010; 22(7):1452–1464. [PubMed: 19583475]

67. Ehrlichman RS, Maxwell CR, Majumdar S, Siegel SJ. Deviance-elicited changes in event-related potentials are attenuated by ketamine in mice. J Cogn Neurosci. 2008; 20(8):1403–1414. [PubMed: 18303985]

68. Hamm JP, Yuste R. Somatostatin Interneurons Control a Key Component of Mismatch Negativity in Mouse Visual Cortex. Cell reports. 2016; 16(3):597–604. [PubMed: 27396334]

69. Jones EG. A new view of specific and nonspecific thalamocortical connections. Adv Neurol. 1998; 77:49–71. discussion 72–43. [PubMed: 9709817]

70. Jones EG. Thalamic organization and function after Cajal. Prog Brain Res. 2002; 136:333–357. [PubMed: 12143393]

71. Jones EG. Synchrony in the interconnected circuitry of the thalamus and cerebral cortex. Ann N Y Acad Sci. 2009; 1157:10–23. [PubMed: 19351352]

72. Viaene AN, Petrof I, Sherman SM. Synaptic properties of thalamic input to layers 2/3 and 4 of primary somatosensory and auditory cortices. J Neurophysiol. 2011; 105(1):279–292. [PubMed: 21047937]

73. Hu B. Functional organization of lemniscal and nonlemniscal auditory thalamus. Exp Brain Res. 2003; 153(4):543–549. [PubMed: 12937877]

74. Cacciaglia R, Escera C, Slabu L, Grimm S, Sanjuan A, Ventura-Campos N, et al. Involvement of the human midbrain and thalamus in auditory deviance detection. Neuropsychologia. 2015; 68:51–58. [PubMed: 25556848]

75. Fruhholz S, van der Zwaag W, Saenz M, Belin P, Schobert AK, Vuilleumier P, et al. Neural decoding of discriminative auditory object features depends on their socio-affective valence. Social cognitive and affective neuroscience. 2016

76. Choi JW, Lee JK, Ko D, Lee GT, Jung KY, Kim KH. Fronto-temporal interactions in the theta-band during auditory deviant processing. Neurosci Lett. 2013; 548:120–125. [PubMed: 23769731]

77. Oates PA, Kurtzberg D, Stapells DR. Effects of sensorineural hearing loss on cortical event-related potential and behavioral measures of speech-sound processing. Ear Hear. 2002; 23(5):399–415. [PubMed: 12411773]

78. Martin BA, Sigal A, Kurtzberg D, Stapells DR. The effects of decreased audibility produced by high-pass noise masking on cortical event-related potentials to speech sounds/ba/and/da. J Acoust Soc Am. 1997; 101(3):1585–1599. [PubMed: 9069627]

79. Molholm S, Martinez A, Ritter W, Javitt DC, Foxe JJ. The neural circuitry of pre-attentive auditory change-detection: an fMRI study of pitch and duration mismatch negativity generators. Cereb Cortex. 2005; 15(5):545–551. [PubMed: 15342438]

80. Fair DA, Schlaggar BL, Cohen AL, Miezin FM, Dosenbach NU, Wenger KK, et al. A method for using blocked and event-related fMRI data to study “resting state” functional connectivity. Neuroimage. 2007; 35(1):396–405. [PubMed: 17239622]

81. Glasser MF, Coalson TS, Robinson EC, Hacker CD, Harwell J, Yacoub E, et al. A multi-modal parcellation of human cerebral cortex. Nature. 2016

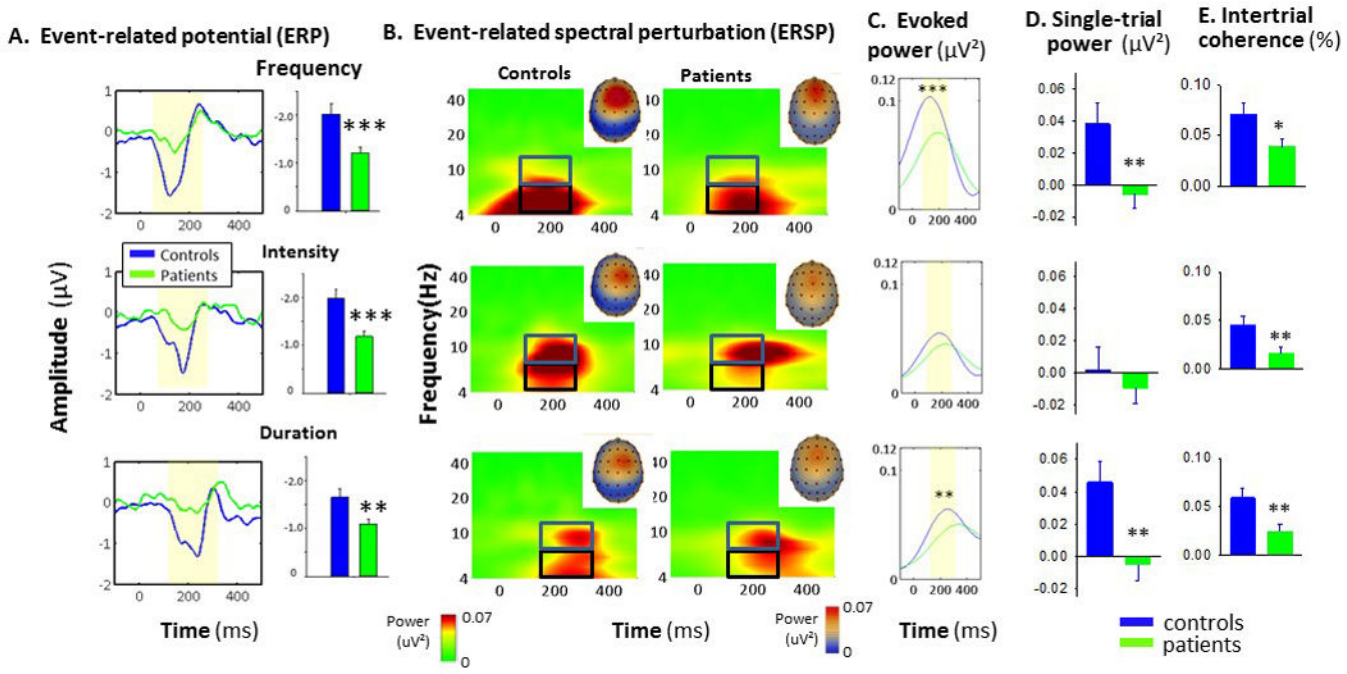

Figure 1.

A. Event-related potential (ERP) waveforms and mean amplitude (bars) to frequency, intensity and duration deviant stimuli. *B.* Event-related spectral perturbation (ERSP) responses as a function of time across frequencies (note log scale). Insets show scalp distribution of MMN-related activity. Boxes show alpha (blue) and theta (black) frequency bins. *C.* Evoked theta power over time. Shaded region represents area of integration. D. Single-trial power within theta frequency band to indicated deviants *E.* Intertrial coherence (ITC) within theta frequency band in controls vs. patients to indicated deviants. *p<.05, **p<.01, ***p<.001 based upon between group t-test

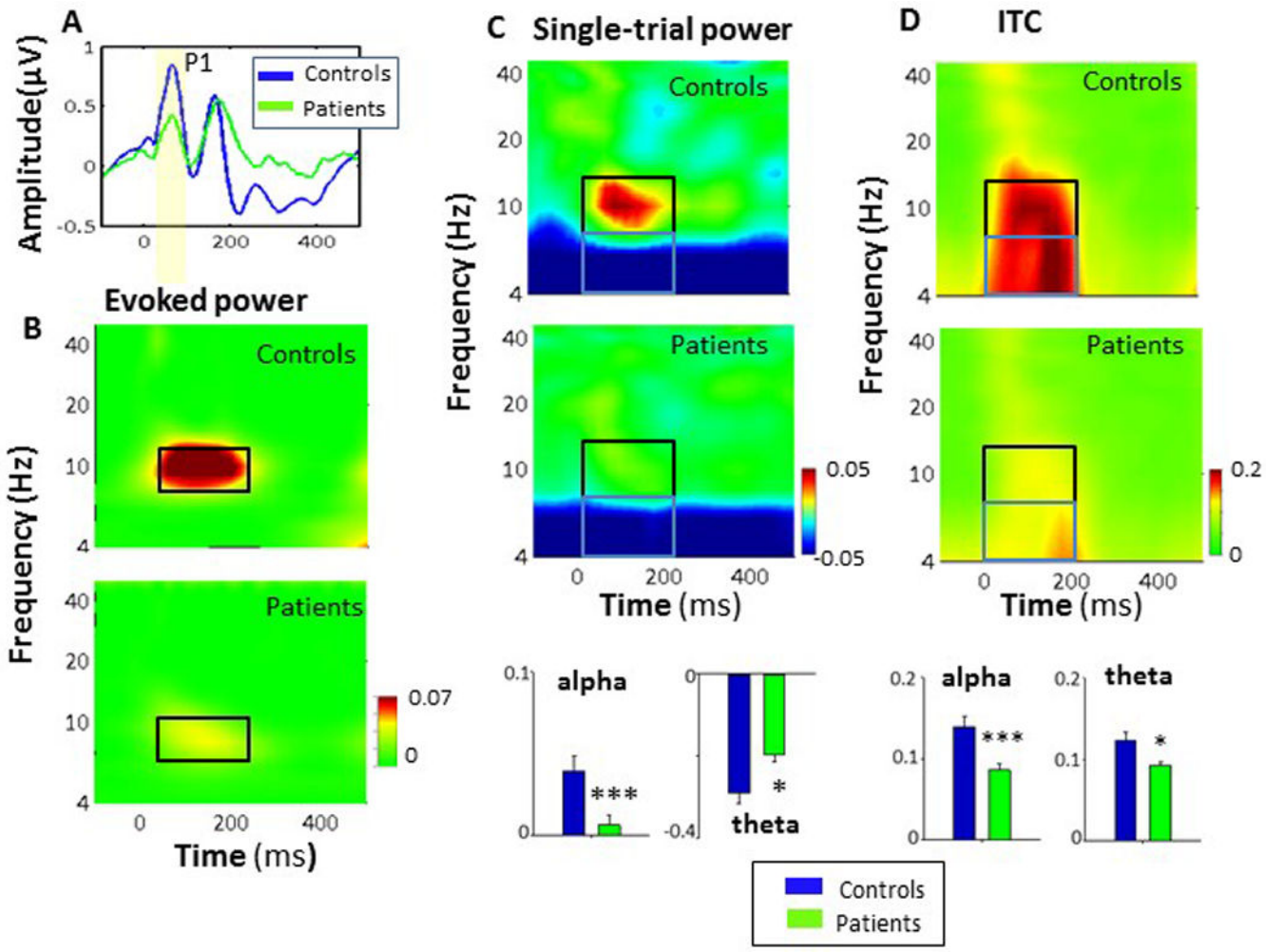

Figure 2.

A. ERP ("time domain") responses to standard stimuli, showing the P1 potential. ***B***. ERSP decomposition response to standards showing the response confined primarily to the alpha-frequency band for both controls and patients, and reduced alpha power in patients vs. controls. ***C***. Single-trial power to standard stimuli, showing a stimulus-induced increase in alpha response and theta inhibition in controls, and reduced change in patients. ***D***. Intertrial coherence (ITC) within alpha (black) and theta (blue) frequency ranges, and bar charts showing values for controls and patients

*p<.05, **p<.01, ***p<.001 based upon between group t-test

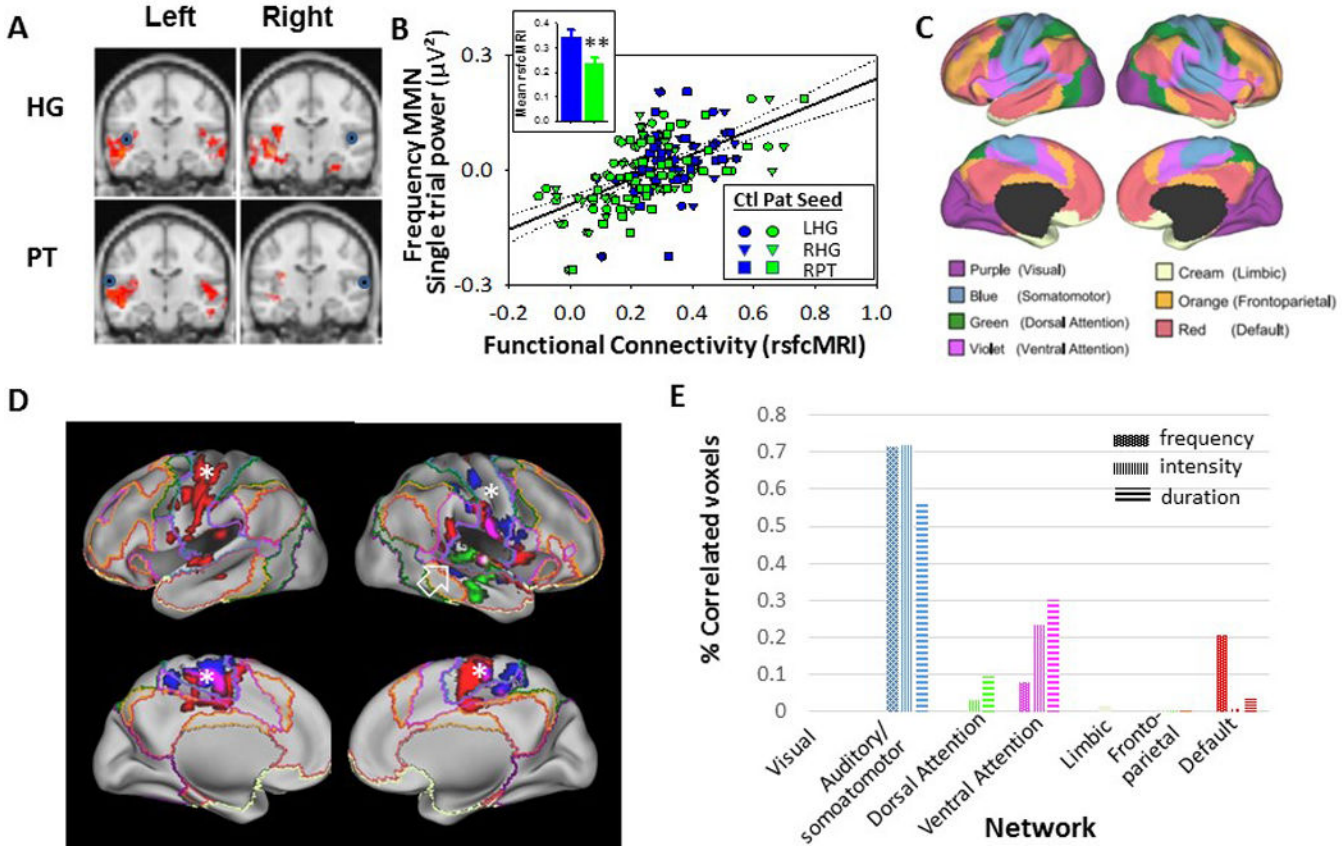

Figure 3.

A. Group-difference maps (red shading) for rsfcMRI connectivity between indicated region and seeds placed in right and left Heschl's gyrus (HG) and planum temporale (PT). Seed locations are shown with blue circles. Data were thresholded at p<.05 corrected for whole brain analysis. *B*. Correlation between indicated functional connectivity regions and theta single-trial power increases to frequency deviant stimuli across seed locations. *Inset:* Between-group difference in rsfcMRI connectivity between HG/PT seeds and auditory correlation region. *C*. functional connectivity networks adapted from the Human Connectome Project[37], based upon the cortical parcellation approach[81]. D. Correlation network for HG seeds mapped onto canonical networks for frequency (green), intensity (red) and duration (blue) deviants. Note localization of networks related to frequency MMN generation primarily to auditory regions (open arrow), vs. more distributed networks involved in intensity/duration MMN (asterisks) *E*. Percentage of voxels by canonical networks showing correlation to HG/PT seeds for frequency, intensity and duration deviants. Percentages were adjusted for relative size of each network

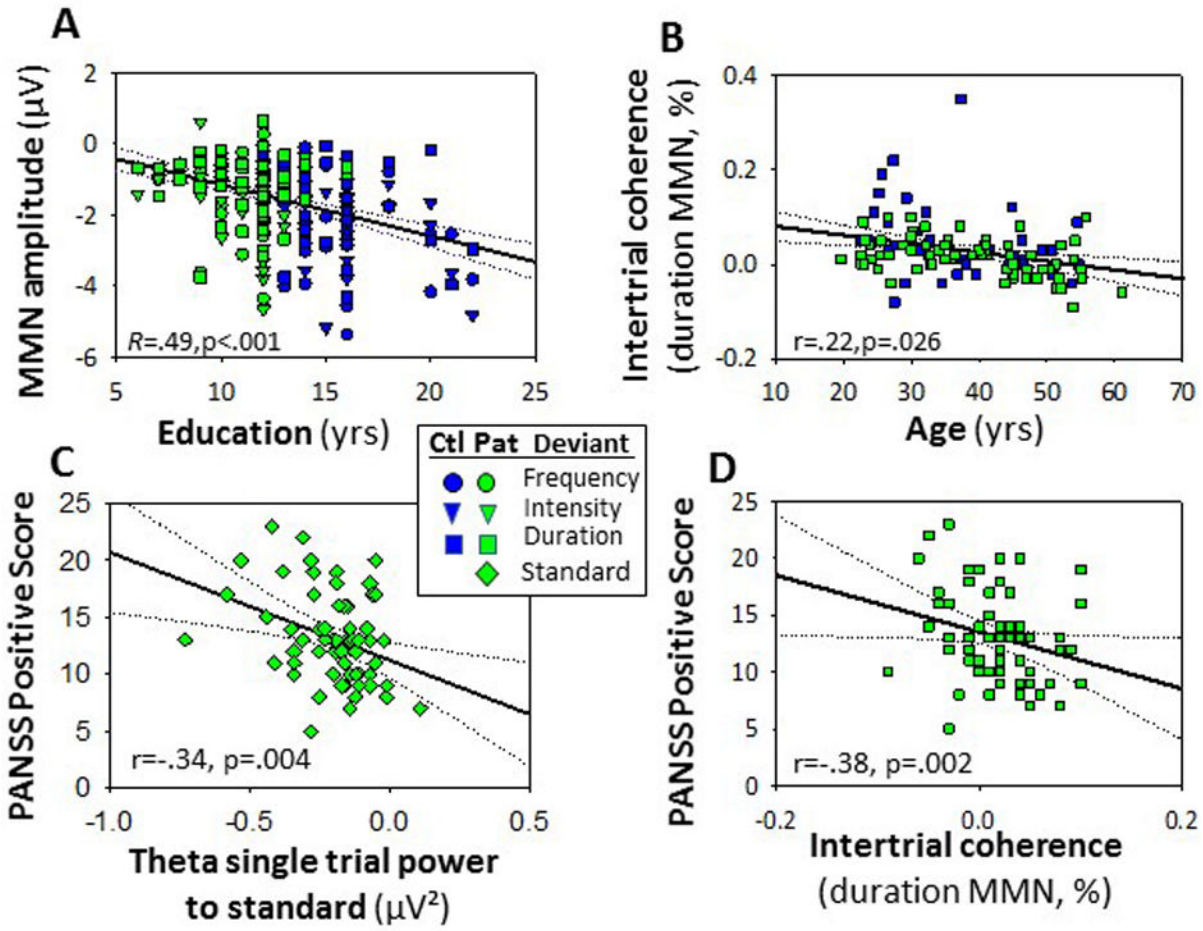

Figure 4.

A. Correlation between years of education completed and MMN amplitude to indicated deviants. *B*. Correlation between ITC response to duration deviants and age. *C*. Level of PANSS positive symptoms as a function of stimulus-induced theta suppression. *D*. Level of PANSS positive symptoms as a function of ITC to duration deviant stimuli.

Table 1

Subject Demographics

	Controls(n=38)	Patients(n=69)
Age	36.26 ± 10.00	39.63 ± 10.78
Gender(M/F)	31/7	66/3
Highest education achieved (yrs)	15.16 ± 2.61** (n=36)	11.23 ± 2.01** (n=56)
Participant socioeconomic status	44.52 ± 13.47 (n=29)	23.71 ± 7.94** (n=48)
Parental socioeconomic status	43.78 ± 14.53 (n=29)	39.04 ± 15.43 (n=40)
Age at first hospitalization(yrs)		21.49 ± 7.69 (n=60)
Illness duration(yrs)		16.76 ± 10.14 (n=60)
Chlorpromazine total(mg)		991.61 ± 821.17 (n=53)
PANSS positive symptom score		12.90 ±4.00 (n=52)
PANSS negative symptom score		14.84 ± 4.91 (n=52)
PANSS cognitive symptom score		11.15 ± 3.74 (n=52)
PANSS excitement symptom score		8.39 ± 3.11 (n=52)
PANSS depressive symptom score		12.13 ±3.36 (n=52)
ILS-PB		38.73 ± 11.88 (n=51)
GAF		43.95 ± 11.00 (n=51)